

Synthesis and characterization of activated carbon derived from date palm leaves

Mubinul Islam^a, Md. Islam^a*, Hemant Mittal^a, Saeed Alhassan^a

^a Khalifa University of Science and Technology, Abu Dhabi, UAE

Abstract

The use of agricultural waste for the production of activated carbon has gained popularity due to the high carbon content of the raw materials, improve sustainability of the product, and low cost. In this paper, activated carbon (DL-AC) was synthesized from discarded date palm leaves. The activation was done via chemical activation where KOH was used as the activating agent. The final product was characterized using XRD and SEM. The XRD results showed a loss in crystallinity due to the activation process whereas the SEM images showed improved porosity of the activated carbon. Water adsorption studies were carried out at 25 °C and the results were fitted to different isotherm models. The adsorption isotherm reported a maximum adsorption capacity of 0.109 g_{wat}/g_{ads} at 0.66 p/p₀. The multilayer adsorption behavior is best explained using the GAB and FHH isotherm models.

Keywords: Activated carbon; Date palm leaves; Water adsorption

1. Introduction

The use of activated carbon in various applications, such as water treatment and gas purification, has led researchers to synthesize the material from different sources and optimize the material based on different parameters such as the type of precursor. Activated carbon is a general term used to define a carbonaceous amorphous material with high porosity, high physiochemical stability, and high adsorption capacity [1]. The increased awareness of climate change has also renewed researchers' interest in the use of activated carbon for carbon capture technologies [2]. While traditional sources for activated carbon are coal and petroleum residues, the use of agricultural waste has led to the cheaper and more sustainable production of activated carbon.

Activated carbon can be prepared using both natural and synthetic precursors, the type and structure of the precursor have an impact on the quality, material characteristics, and general capacity of the product [3]. Previously researchers have made use of raw materials such as hazelnut shells [4], olive stones [5], coconut shells [6], wood [7], rice husk [8], bamboo [9], and many more. The choice of raw materials was primarily based on

availability and affordability. Researchers have also optimized the activated carbon based on temperature, activating agent, and additional modifications post-synthesis. In their paper, Rahma et al. investigated the impact of using two different activating agents, KOH and ZnCl₂ on the surface area and morphological properties of the activated carbon derived from corncob waste [10]. Studies have also focused on the specific applications of agricultural waste-derived activated carbon. Deng et al. have reported in their work the synthesis of activated carbon from peanut and sunflower seed shells for the adsorption of CO₂ from the atmosphere [11]. Ridassepri et al. have synthesized activated carbon from Bagasse waste for atmospheric water vapor adsorption and optimized the material at different activation temperatures [12].

A previous study on the synthesis of biochar from date palm leaves was conducted and the material was assessed for its carbon capture properties [13]. The authors reported that the cultivation of date palm trees in the UAE results in huge agricultural waste in the country, with about 20 kg per tree per year. The synthesis method followed a simple pyrolysis procedure at different temperatures with no activating agents used. In this paper, we synthesize activated carbon from date palm leaves using chemical activation where KOH was used as the activating agent. The material is characterized using x-ray

* Corresponding author. Tel.: +971 2 312 3244

Fax: +971 2 312 3244; E-mail: didarul.islam@ku.ac.ae

© 2016 International Association for Sharing Knowledge and Sustainability

DOI: 10.5383/ijtee.19.02.005

diffraction (XRD) and scanning electron microscopy (SEM) to assess the morphological and crystalline properties. The water adsorption capacity of the material is also studied at 25 °C and different isotherm models were fitted to the experimental data. The water adsorption capacity is an important parameter to assess both the feasibility of the material in desiccant applications and the hydrophobicity of the material in gas separation and purification applications [14].

2. Synthesis and methodology

2.1. Synthesis

Discarded date palm tree branches were collected from private gardens in Abu Dhabi/UAE and the leaves were removed by cutting the leaf buds. The leaves were washed thoroughly and left in an oven at 100 °C for 24 hours or until completely void of moisture. The dried leaves were cut into small pieces (1-2 cm size) and then ground and sieved into a fine powder (50 μm) using the Biolomix lab grinder. The resulting powder was then put in a closed crucible and placed inside a Nabertherm box furnace to be carbonized at 600 °C for 2 hours at a ramp-up rate of 10 °C/min. This process results in the formation of nonporous carbon (NC). The NC powder is washed using deionized (DI) water and dried to remove any water-soluble impurities. It is then mixed in approximately 50ml DI water along with potassium hydroxide (KOH) at a ratio of 2:1, where 2 grams of KOH was used for every gram of NC. The mixture was stirred continuously while being heated at 90 °C until most of the water evaporates, the final solution is placed in an oven at 100 °C to completely dry the mixture. The resulting powder was placed in the furnace and heated at 800 °C for 5 hours at a ramp-up rate of 5 °C/min. At this temperature, the activation process starts wherein the KOH reacts with the carbon structure of the NC material making the final product porous, and thus date palm leaf-derived activated carbon (DL-AC) is produced. The overall reaction of the KOH with the carbon structure is as follows [15]:

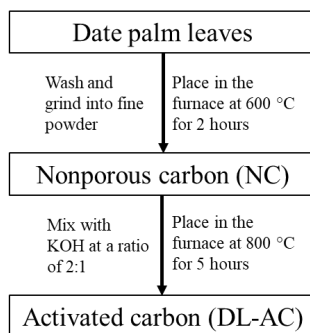
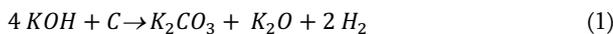


Fig. 1: Flow chart summarizing the synthesis process

2.2. Characterization

The two samples, nonporous carbon (NC) and activated carbon (DL-AC), were characterized to understand the effect of the activation process. X-ray diffraction patterns (XRD) were studied using the Bruker D2 phase instrument with the 2θ range set from 5° to 90° at an increment of 0.1°. The formation of pores and morphological changes due to the activation process is studied using the Quanta 250 scanning electron microscopy (SEM) machine. The samples were attached to aluminium studs using carbon tapes and the study was conducted under vacuum conditions.

2.3. Water adsorption studies

To quantify the adsorption capacity at a constant temperature, the adsorption studies were carried out with increasing relative pressures. The experiment was done at 25 °C using the Rubotherm vapor dosing system (VDS). The experimental data was analysed using the following isotherm models:

1. Freundlich isotherm and is written per Eq. 2 as:

$$q = k_F (a_w)^{\frac{1}{n}} \quad (2)$$

Where q is the vapor adsorbed, a_w is the relative humidity, k_F is the equilibrium constant and n is the adsorption intensity. This isotherm assumes several layers of adsorbate and a nonhomogeneous adsorption process [16].

2. Brunauer, Emmett and Teller (BET) isotherm which disrobed in Eq. 3 as:

$$q = \frac{q_m c a_w}{(1 - a_w)(1 + (c - 1)a_w)} \quad (3)$$

Where q is the vapor adsorbed, a_w is the relative humidity, q_m is the maximum monolayer adsorption capacity and c is the BET constant. Assumes multilayer adsorption process and is one of the most used models [17].

3. Guggenheim, Anderson, and Boer (GAB) isotherm and is written in Eq. 4 as:

$$q = \frac{q_m c_G k_G a_w}{(1 - k_G a_w)(1 - k_G a_w + c_G k_G a_w)} \quad (4)$$

Where q is the vapor adsorbed, a_w is the relative humidity, q_m is the maximum monolayer adsorption capacity, and c_G and k_G are the GAB constants. The isotherm extension of the BET model to consider wider relative pressures [18].

4. Frenkel-Halsey-Hill (FHH) isotherm which is described in Eq. 5 as:

$$q = q_m [-\ln(a_w)]^{\frac{-1}{r}} \quad (5)$$

Where q is the vapor adsorbed, a_w is the relative humidity, q_m is the maximum monolayer adsorption capacity, r is the FHH constant, and $1/r$ represents the nature of interactions between the solid surface [17].

5. Langmuir isotherm and it is written in Eq. 6 as:

$$q = \frac{q_m b a_w}{1 + b a_w} \quad (6)$$

Where q is the vapor adsorbed, a_w is the relative humidity, q_m is the maximum monolayer adsorption capacity, b is the Langmuir constant [17].

3. Results and discussion

3.1. X-ray diffraction (XRD)

For the nonporous carbon (NC), sharp peaks are observed at around 28° and 40° as shown in Figure 2. These are the crystalline peaks of biomass-based carbon materials such as date

palm leaves derived carbon [10]. The XRD peaks for the DL-AC sample is shown in Figure 3, where one can notice an absence of any sharp peaks. The activation process results in the degradation of the crystalline structure due to the formation of pores. Therefore, the material can be termed amorphous.

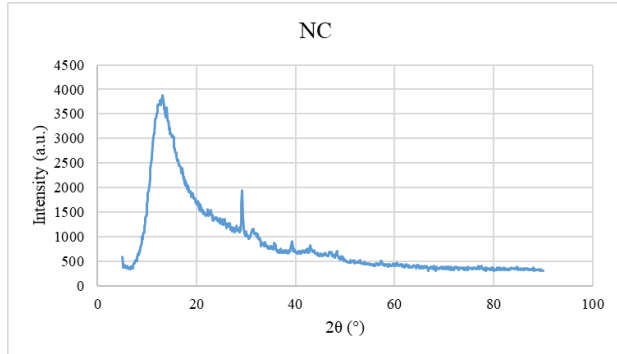


Fig. 2: Sharp peaks show the crystalline structure of the NC

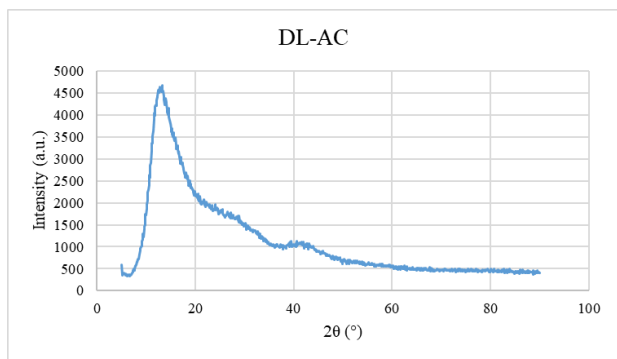


Fig. 3: The absence of peaks show that the material is amorphous

3.2. Scanning electron microscopy (SEM)

In Figure 4 a) – c), the SEM images of the NC sample is shown where we see fewer number of pores. When comparing this to the DL-AC sample in Figure 4 d) – e), the number of pores in the DL-AC is shown to be higher. This is due to the pore widening effect that occurs when the KOH disintegrates at high temperature during the activation process [19].

3.3. Adsorption isotherm

The water adsorption isotherm for the DL-AC sample is shown in Figure 5 and it follows a type V isotherm as per the IUPAC [20]. This behaviour is common for water vapor adsorption on activated carbon materials and shows an increasing adsorption capacity with increasing relative pressure. The initial adsorption happens due to the attachment of the water molecules to the surface of the material through interactions with surface functional groups [21]. As the relative pressure increases the water molecules interact with each other to form clusters which eventually diffuse into the pores, this phenomenon is sometimes known as the pore-filling mechanism [12, 21]. The adsorption capacity never reaches saturation throughout the study, this is evidence of the material's robust properties [22]. The maximum adsorption capacity is $0.109 \text{ g}_{\text{wat}}/\text{g}_{\text{ads}}$ at 0.66 p/p_0 .

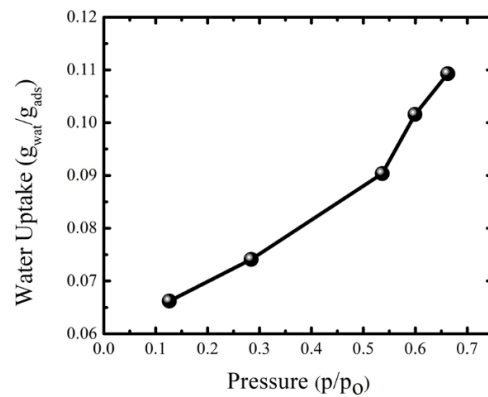


Fig. 4: Water adsorption isotherm of the DL-AC sample showing a type V behavior

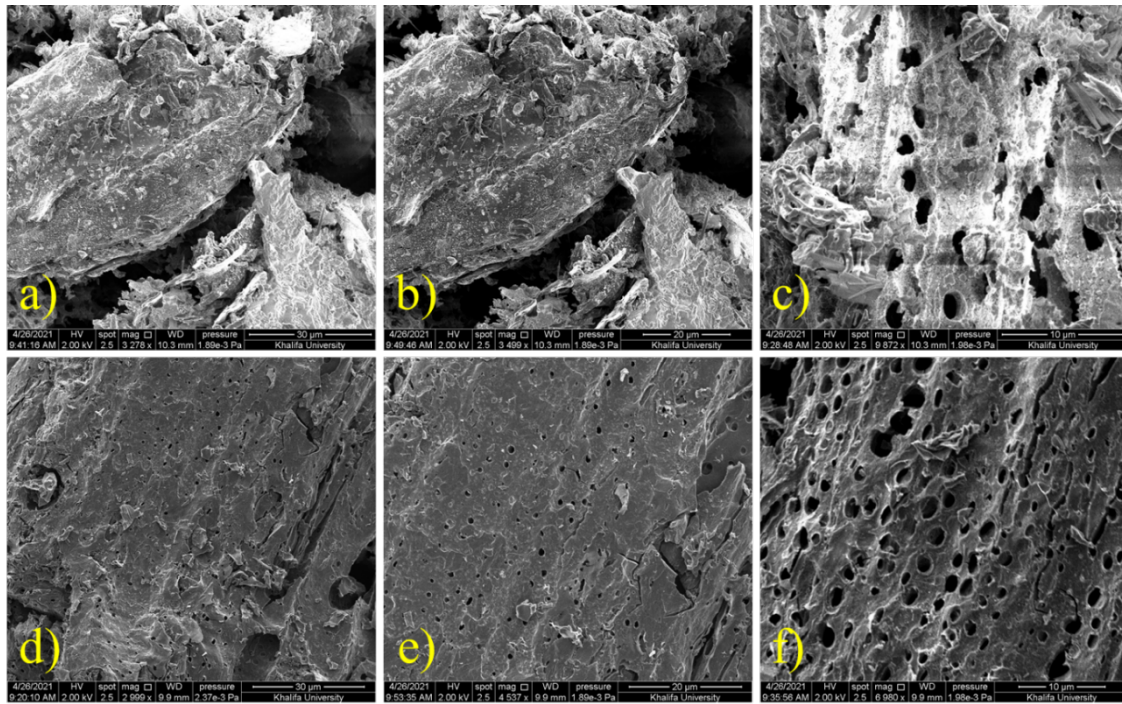


Fig. 5: a) – c) SEM images showing relatively smooth surface of the sample, d) – f) SEM images showing the increased porosity of the sample

The data from the isotherm experiment was fitted to the five isotherm models and the plots are shown in Figure 6. Based on the error calculation using reduced chi-square and coefficient of determination, the GAB and FHH isotherms were found to be the best-fitting model.

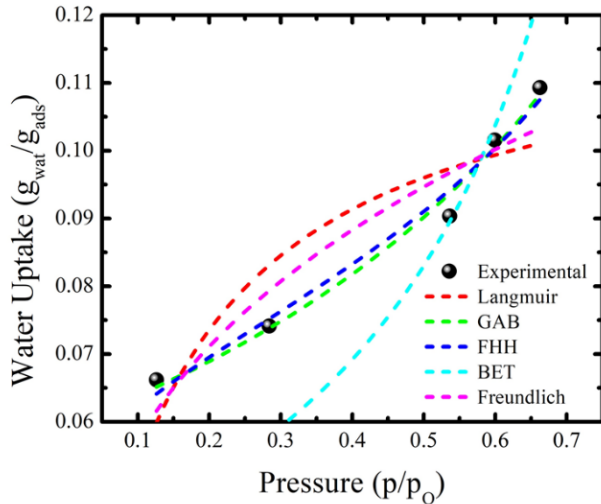


Fig. 6: Isotherm model fits for the experimental data

Both the GAB and FHH were reasonably able in explaining the multilayer adsorption behavior of the material. The cluster formation on the activated carbon leads to layers of water molecules interacting with each other until pore condensation occurs [21]. The GAB model has a higher fitting parameter since it considers wider partial pressures [18]. The model parameters for all the isotherm models are shown in Table 1.

Table 1: Isotherm model parameters for DL-AC sample

Isotherm model	Parameter	DL-AC 25 °C
Freundlich	k_F	0.11753
	n	3.20476
	Red. X^2	4.2193×10^{-5}
	R^2	0.87126
BET	$q_m (g_{wat}/g_{ads})$	0.04151
	c	3.13337×10^{44}
	Red. X^2	2.67368×10^{-4}
	R^2	0.18419
GAB	$q_m (g_{wat}/g_{ads})$	0.05957
	c_G	1.20175×10^{44}
	k_G	0.67906
	Red. X^2	7.25539×10^{-6}
	R^2	0.97786
FHH	$q_m (g_{wat}/g_{ads})$	0.08096
	r	3.12233
	Red. X^2	8.24443×10^{-6}
	R^2	0.97484
Langmuir	$q_m (g_{wat}/g_{ads})$	0.12057
	b	7.81765
	Red. X^2	8.08879×10^{-5}
	R^2	0.75319

4. Conclusion

Researchers have increasingly focused on the use of sustainable raw materials for the synthesis of different adsorbents. These materials are usually employed in the treatment of polluted waters and the removal of harmful gases from the atmosphere. Therefore, it is imperative that the manufacturing process of these materials have a low carbon footprint. One way to ensure such compliance is to use agricultural waste as raw material for these adsorbents. The synthesis of activated carbon from date palm leaves using KOH as the activated agent resulted in a sustainable and relatively inexpensive adsorbent. The activation process resulted in a loss in crystallinity due to improved porosity which is observed in the absence of XRD peaks. The adsorption isotherm shows a type V behavior, which denotes a versatile material with hydrophobic properties at low relative pressure and hydrophilic properties at high relative pressure. The experimental data were modeled using different isotherm models which showed that the multilayer adsorption behavior of the activated carbon is well explained by the GAB and FHH isotherm models. The results in this paper demonstrate the feasibility of using date palm leaf-derived activated carbon in different adsorption applications.

Nomenclature

NC	Nonporous carbon
XRD	X-ray Diffraction
SEM	Scanning Electron Microscope
DL-AC	Date palm leaf-derived activated carbon
g_{wat}/g_{ads}	Grams of water per gram of adsorbent

Acknowledgments

The support received from Khalifa University of Science and Technology to carry out this work is highly acknowledged.

References

- [1] M. Al-Sarraf and M. Abbas, "PREPARATION OF ACTIVATED CARBON FROM SUNFLOWER SEEDS," 2020.
- [2] A. Alabadi, S. Razzaque, Y. Yang, S. Chen, and B. Tan, "Highly porous activated carbon materials from carbonized biomass with high CO₂ capturing capacity," *Chemical Engineering Journal*, vol. 281, pp. 606–612, 2015, doi: 10.1016/j.ccej.2015.06.032.
- [3] M. A. Yahya, Z. Al-Qodah, and C. W. Z. Ngah, "Agricultural bio-waste materials as potential sustainable precursors used for activated carbon production: A review," *Renewable and Sustainable Energy Reviews*, vol. 46, pp. 218–235, 2015, doi: 10.1016/j.rser.2015.02.051.
- [4] Y. Örkün, N. Karatepe, and R. Yavuz, "Influence of temperature and impregnation ratio of H₃PO₄ on the production of activated carbon from hazelnut shell," *Acta Phys Pol A*, vol. 121, no. 1, pp. 277–280, 2012, doi: 10.12693/APhysPolA.121.277.
- [5] R. Ubago-Pérez, F. Carrasco-Marín, D. Fairén-Jiménez, and C. Moreno-Castilla, "Granular and monolithic activated carbons from KOH-activation of olive stones," *Microporous and Mesoporous Materials*, vol. 92, no. 1–3, pp. 64–70, 2006, doi: 10.1016/j.micromeso.2006.01.002.
- [6] W. Li, K. Yang, J. Peng, L. Zhang, S. Guo, and H. Xia, "Effects of carbonization temperatures on characteristics of

- porosity in coconut shell chars and activated carbons derived from carbonized coconut shell chars,” *Ind Crops Prod*, vol. 28, no. 2, pp. 190–198, 2008, doi: 10.1016/j.indcrop.2008.02.012.
- [7] Yusufu M. I., “Production and characterization of activated carbon from selected local raw materials,” *African Journal of Pure and Applied Chemistry*, vol. 6, no. 9, pp. 123–131, 2012, doi: 10.5897/ajpac12.022.
- [8] N. Yalçın and V. Sevinç, “Studies of the surface area and porosity of activated carbons prepared from rice husks,” *Carbon N Y*, vol. 38, no. 14, pp. 1943–1945, 2000, doi: 10.1016/S0008-6223(00)00029-4.
- [9] F. Ademiluyi, S. Amadi, and N. Amakama, “Adsorption and Treatment of Organic Contaminants using Activated Carbon from Waste Nigerian Bamboo,” *Journal of Applied Sciences and Environmental Management*, vol. 13, no. 3, 2010, doi: 10.4314/jasem.v13i3.55351.
- [10] N. A. Rahma, A. Kurniasari, Y. D. Setyo Pambudi, H. M. Bintang, A. Zulfia, and C. Hudaya, “Characteristics of Corn-cob-Originated Activated Carbon Using Two Different Chemical Agent,” *IOP Conf Ser Mater Sci Eng*, vol. 622, no. 1, 2019, doi: 10.1088/1757-899X/622/1/012030.
- [11] S. Deng et al., “Activated carbons prepared from peanut shell and sunflower seed shell for high CO₂ adsorption,” *Adsorption*, vol. 21, no. 1–2, pp. 125–133, Feb. 2015, doi: 10.1007/s10450-015-9655-y.
- [12] A. F. Ridassepri, F. Rahmawati, K. R. Heliani, Chairunnisa, J. Miyawaki, and A. T. Wijayanta, “Activated carbon from bagasse and its application for water vapor adsorption,” *Evergreen*, vol. 7, no. 3, pp. 409–416, 2020, doi: 10.5109/4068621.
- [13] I. ben Salem, M. el Gamal, M. Sharma, S. Hameedi, and F. M. Howari, “Utilization of the UAE date palm leaf biochar in carbon dioxide capture and sequestration processes,” *J Environ Manage*, vol. 299, no. July, p. 113644, 2021, doi: 10.1016/j.jenvman.2021.113644.
- [14] X. L. Yao, L. Q. Li, H. L. Li, and W. W. Ma, “A simplified adsorption model for water vapor adsorption on activated carbon,” *J Cent South Univ*, vol. 21, no. 4, pp. 1434–1440, 2014, doi: 10.1007/s11771-014-2082-5.
- [15] Z. Heidarnejad, M. H. Dehghani, M. Heidari, G. Javedan, I. Ali, and M. Sillanpää, “Methods for preparation and activation of activated carbon: a review,” *Environmental Chemistry Letters*, vol. 18, no. 2. Springer, pp. 393–415, Mar. 01, 2020. doi: 10.1007/s10311-019-00955-0.
- [16] M. El-Dairi et al., “Adsorption,” *Alliances : Re/envisioning Indigenous-non-indigenous Relationships*, vol. 25, no. ii, pp. 11–28, 2014.
- [17] M. A. Al-Ghouti and D. A. Da’ana, “Guidelines for the use and interpretation of adsorption isotherm models: A review,” *Journal of Hazardous Materials*, vol. 393. Elsevier B.V., Jul. 05, 2020. doi: 10.1016/j.jhazmat.2020.122383.
- [18] H. Mittal, A. al Alili, and S. M. Alhassan, “Adsorption isotherm and kinetics of water vapors on novel superporous hydrogel composites,” *Microporous and Mesoporous Materials*, vol. 299, Jun. 2020, doi: 10.1016/j.micromeso.2020.110106.
- [19] H. M. Yang, D. H. Zhang, Y. Chen, M. J. Ran, and J. C. Gu, “Study on the application of KOH to produce activated carbon to realize the utilization of distiller’s grains,” *IOP Conf Ser Earth Environ Sci*, vol. 69, no. 1, 2017, doi: 10.1088/1755-1315/69/1/012051.
- [20] X. Zheng, T. S. Ge, and R. Z. Wang, “Recent progress on desiccant materials for solid desiccant cooling systems,” *Energy*, vol. 74, no. 1. Elsevier Ltd, pp. 280–294, 2014. doi: 10.1016/j.energy.2014.07.027.
- [21] S. Sun, Q. Yu, M. Li, H. Zhao, and C. Wu, “Preparation of coffee-shell activated carbon and its application for water vapor adsorption,” *Renew Energy*, vol. 142, pp. 11–19, 2019, doi: 10.1016/j.renene.2019.04.097.
- [22] G. Singh, K. S. Lakhi, C. I. Sathish, K. Ramadass, J. H. Yang, and A. Vinu, “Oxygen-Functionalized Mesoporous Activated Carbons Derived from Casein and Their Superior CO₂ Adsorption Capacity at Both Low- And High-Pressure Regimes,” *ACS Appl Nano Mater*, vol. 2, no. 3, pp. 1604–1613, Mar. 2019, doi: 10.1021/acsanm.9b00059.